N73-14985

NASA TECHNICAL MEMORANDUM

NASA TM X-2696

NASA TM X-2696

CASE FILE COPY

SOME OBSERVED EFFECTS OF PART-SPAN DAMPERS ON ROTATING BLADE ROW PERFORMANCE NEAR DESIGN POINT

by Genevieve M. Esgar and Donald M. Sandercock

Lewis Research Center
Cleveland, Ohio 44135

NATIONAL AERONAUTICS AND SPACE ADMINISTRATION • WASHINGTON, D. C. • JANUARY 1973

1. Report No.	2. Government Accession No.	3. Recipient's Catalog No.
NASA TM X-2696		

4. Title and Subtitle	5. Report Date
SOME OBSERVED EFFECTS OF PART-SPAN DAMPERS ON ROTATING BLADE ROW PERFORMANCE NEAR DESIGN POINT	January 1973
	6. Performing Organization Code

7. Author(s)	8. Performing Organization Report No.
Genevieve M. Esgar and Donald M. Sandercock	E-7067
	10. Work Unit No. 501-24

9. Performing Organization Name and Address	11. Contract or Grant No.
Lewis Research Center National Aeronautics and Space Administration Cleveland, Ohio 44135	
	13. Type of Report and Period Covered: Technical Memorandum

12. Sponsoring Agency Name and Address	14. Sponsoring Agency Code
National Aeronautics and Space Administration Washington, D.C. 20546	

15. Supplementary Notes

16. Abstract

Detailed measured radial distributions of flow parameters for eight rotors with part-span dampers are used to study the effects of dampers on rotor performance and flow parameters at near design operation. All rotors had a blade tip diameter of about 50.8 centimeters (20 in.) and operated at a blade tip speed of about 426.7 meters per second (1400 ft/sec). Several examples demonstrate that, when the local loss variations in the damper flow region are included in an aerodynamic design or analysis procedure, the computed spanwise distributions of flow parameters compare closely with measured distributions.

17. Key Words (Suggested by Author(s))	18. Distribution Statement
Transonic axial flow compressor rotor Damper effect on performance Loss correlation	Unclassified - unlimited

19. Security Classif. (of this report)	20. Security Classif. (of this page)	21. No. of Pages	22. Price*
Unclassified	Unclassified	26	$3.00

* For sale by the National Technical Information Service, Springfield, Virginia 22151

SOME OBSERVED EFFECTS OF PART-SPAN DAMPERS ON ROTATING BLADE ROW PERFORMANCE NEAR DESIGN POINT

by Genevieve M. Esgar and Donald M. Sandercock

Lewis Research Center

SUMMARY

Measurements of the radial distributions of flow conditions at the inlet and outlet of a number of high-rotative-speed rotors have sufficient detail to define flow conditions in the blade part-span damper flow region. Data near the design operating point of eight of these rotors are presented herein. All rotors had a blade tip diameter of approximately 50.8 centimeters (20 in.) and operated at a blade tip speed of 426.7 meters per second (1400 ft/sec). The damper geometry did not vary over a wide range, but the data indicated some qualitative effects of a damper on the radial distributions of flow that should be generally applicable. The data also provides a base for estimating the quantitative effects of the damper at flow conditions and geometries differing from those reported herein.

The radial distributions of flow parameters indicated an increase in loss and blade loading and a decrease in fluid turning and axial velocity (flow) immediately downstream of the damper. The most direct effects appeared to occur over a spanwise distance of about 10 times the damper maximum thickness. Some lesser effects occur at all spanwise locations due to radial equilibrium requirements.

Several examples are presented to demonstrate that when the local loss variation through the damper flow region are applied in an aerodynamic design or analysis program, the computed results compare closely with measured spanwise distributions.

INTRODUCTION

Two means for decreasing compressor weight, a continuous goal of compressor research, are increasing the pressure producing capability of the individual stages and using short chord blading. This, in turn, leads to high-aspect-ratio blades (AR = ratio of blade span to blade chord) rotating at very high speed. In order to satisfy mechanical

integrity (in particular, to keep aeroelastic instabilities within known safe limits) of these high-speed, high-aspect-ratio blades mechanical designers have linked adjacent blades by means of so-called "part-span dampers."

The part-span dampers have a measurable, but not well defined, effect on the aerodynamic performance of a stage. This is generally recognized by applying gross corrections to blade row efficiency and flow blockage in design procedures.

At the NASA Lewis Research Center a number of single-stage experimental studies have used rotor blading with part-span dampers. In one case the blade row was subsequently modified by reducing the damper size and retested. In the test procedures, sufficient measurements were taken to provide good definition of the radial distributions of flow conditions immediately downstream of the damper.

In this report the radial distributions of selected blade element parameters from eight rotating blade rows with part-span dampers are presented. All data are those measured at design operating speed (blade tip speed, 426.7 m/sec (1400 ft/sec) for all rotors) and near maximum efficiency (design) operation. Some general effects of the dampers on the radial distributions of parameters are discussed. The effects of the dampers on blade-element losses are correlated and several examples, which include the local loss distributions across the damper region in aerodynamic calculation procedures, are presented.

APPARATUS AND PROCEDURES

Test Rotor Blade Rows

Experimental test results from eight rotor configurations have been used in this study. Design parameters and detailed blade geometry for most of the configurations have been reported in references 1 to 7. A summary of rotor blade damper geometry for the eight configurations used in the study is given in table I. The sketch on figure 1 defines the damper geometry parameters given in table I. The values listed on table I are considered to be approximate because, for some configurations, the values were obtained from measurements of fabricated blades. For all configurations the damper was located at approximately 45 percent of the span from the rotor tip.

Compressor Test Facility

A schematic of the general test facility used to test the eight rotor configurations is shown in figure 2. More specific details on the facility as used in the testing of the individual rotors are given in the references.

Instrumentation

Data used in this study were primarily calculated from radial surveys of flow conditions at axial locations within one chord distance upstream and downstream of the rotating blade row. Photographs of typical probes used to measure total and static pressure, total temperature, and flow angle are shown in figure 3. Airflow through the compressor was measured with a thin-plate orifice installed according to ASME standards.

Compressor speed was indicated with the use of a magnetic pickup in conjunction with a gear mounted on the drive motor shaft. All data were measured by an automatic digital potentiometer and recorded on paper tape. The accuracy of the measurements is estimated to be:

Inlet pressure, psi	±0.05
Outlet pressure, psi	±0.10
Temperature, ^{o}R	±1.0
Weight flow, percent	±1.0
Speed, percent	±0.5
Flow angle, deg	±2

Blade-Element Parameters

The blade-element parameters were calculated in accordance with the definitions and equations given in appendices A and B. The blade-element data are based on the calculated flow parameters at planes approximating the blade leading and trailing edges. The translation of flow parameters from the measuring stations to the blade leading- and trailing-edge planes was made using the following assumptions. The actual radii and slopes of the streamlines were assumed to correspond to those of the design streamlines. The total pressure, total temperature, and angular momentum of flow along any given streamline were assumed to be constant between the measuring station and the blade edge. The ratio of the weight flow per unit area (static density times axial velocity) at the measuring station to the weight flow per unit area at the blade edge along any given streamline was assumed to equal the value calculated from the flow parameters in design.

It should be recognized that when applying this data-translation procedure, the form of the wake from the damper as measured at the blade outlet measuring station is translated also to the blade trailing edge. The translation procedure does not allow for any momentum interchange between the measuring and translated station such as occurs in a wake mixing process. No attempt is made herein to quantitatively analyze this effect. Axial distances between the blade trailing edge and the outlet measuring stations fall

within the range of 1.5 to 2.3 centimeters (0.6 to 0.9 in.). Absolute flow angles at rotor exit can be computed from the tangential and meridional flow velocities.

RESULTS AND DISCUSSION

The data and discussion presented herein are limited to operation at design speed and near maximum efficiency. Thus, the damper effects shown are those occurring near design operating conditions.

A blade-element approach is applied to all streamlines in the damper flow region even though it may be questionable whether certain blade-element parameters, as usually defined, apply throughout this flow region. However, most design and analysis procedures require a continuous spanwise input of blade-element parameters. Consequently, the data were presented in terms of the conventional parameters.

In this section the radial distributions of blade-element parameters for all rotors are presented, and some general effects of the dampers on the blade-elements parameters discussed. From this analysis, additional correlations of selected parameters are made. Finally, several aerodynamic design calculations, which include the local effects of the blade part span dampers, are presented.

Overall Performance

In order to illustrate the general performance levels, operating ranges, and location of the maximum efficiency point in the operating range for the rotor blade rows, the overall performances of the rotor blade rows are shown in figure 4. Mass-averaged values of pressure ratio and efficiency are presented as functions of corrected weight flow. The blade tip speed (at blade leading edge) of all rotors is approximately 426.7 meters per second (1400 ft/sec). All rotor rows were approximately 50.8 centimeters (20 in.) in diameter at blade leading edge.

Blade-Element Parameters

The radial distributions of blade-element parameters are presented in figure 5. Definitions of the parameters are given in appendix A.

The overall effects of the midspan damper on the radial distributions of blade-element parameters cannot be completely isolated. Largest, and most direct, effects will be measured immediately downstream of the damper; however, radial equilibrium requirements spread these effects in some degree to all elements along the blade span.

Thus, the performance of a blade row is dependent on both the radial gradient and magnitude of flow parameters.

The qualitative effects of the damper on the radial distributions of the flow and performance parameters are generally apparent from figure 5. Perhaps most significant is the sharp local increase in loss $\bar{\omega}$ in the vicinity of the damper. This, in turn, is primarily responsible for the decrease in through-flow velocity V_M and outlet pressure P_2, or pressure ratio, in this flow region. The damper presence also generally resulted in some small decrease in the fluid turning (as evidenced in fig. 5 by an increase in deviation angle δ) in the damper region. A decrease in fluid turning means a decrease in energy addition (indicated by the outlet tangential velocity $V_{\theta 2}$ in fig. 5 and the relation for each streamline for these rotors, that energy addition equals $U_2 V_{\theta 2}/g$). However, a decrease in outlet through-flow velocity V_M tends to increase energy addition. The combined effect of lower fluid turning and lower through-flow velocity is to maintain (or slightly increase) the energy addition level across the damper flow region. Further, maintaining the energy addition level but increasing the loss level results in a decrease in local efficiency that would tend to be the inverse of the loss distribution.

The most direct illustration of the effects of damper thickness on rotor performance parameters can be obtained by comparing the data of rotors 3A and 3B (figs. 5(a) and (b)). The only change in rotor configuration was the decrease in damper size. However, the rotor 3B configuration was tested with a longer inlet section than that used in the 3A tests, so the casing boundary layer entering the 3B rotor blades was somewhat thicker than that entering the 3A rotor row. The thinner dampers for rotor 3B resulted in lower loss levels, lower D-factors, and a smaller V_M deficit in the damper flow region. However, the losses in the blade tip region of 3B were higher than for 3A so that the overall maximum efficiency did not change. The data from these two configurations is presented and discussed in reference 2.

Damper Loss

In the calculation of aerodynamic parameters, the effects of the part-span damper on flow at the blade-row outlet are accounted for in the radial distributions of loss and fluid turning (deviation angle). The radial distributions of parameters shown in figure 5 indicated that the primary effect of the damper on the blade-element parameters resulted from the additional loss generated in the damper flow region. The remainder of this report is directed to correlating the local loss distributions in the damper flow region and incorporating them into aerodynamic design and analysis methods.

Loss is presented as a profile-loss coefficient $\bar{\omega}_p$ which is obtained by subtracting a shock loss (computed from the methods of ref. 8) from the measured total-loss

coefficient. The profile loss shown includes the loss due to viscous flow over the blade surfaces plus the loss due to secondary (three-dimensional) flows, which occur primarily in the blade end regions. Attempts to clearly identify the portions of the overall loss due to secondary (three-dimensional) flows in rotating blade rows have been generally unsuccessful.

In the design system used on the rotors presented herein, the profile loss coefficient is considered a function of a blade-element loading parameter, the D-factor (D)) only. The three-dimensional flow effects are accounted for by varying the $\overline{\omega}_p$-D relation according to the spanwise location of the blade element. For example, at a given D-factor level, a blade element near the blade tip would have a higher loss coefficient than one in the mean radius region of the blade span. Following this approach, the $\overline{\omega}_p$-D relations (from fig. 5) for (1) blade elements which are relatively unaffected by the three-dimensional flows in blade end and damper flow regions, (2) blade elements 5 percent of span height from the outer wall, and (3) blade elements passing through the maximum loss measurement directly downstream of the damper are plotted in figure 6.

The blade elements that are essentially unaffected by three-dimensional flows show a correlation of $\overline{\omega}_p$ with D within a reasonably narrow band. By comparison, for those elements in blade tip and damper flow regions, the profile loss coefficients are larger and show significant scatter. This is expected because (1) the magnitude of the three-dimensional flows that contribute to the loss levels are a function of additional parameters (casing boundary layer, pressure gradients, blade tip clearances, etc.), and (2) accurate measurements near the casing wall and in the damper wakes are difficult to obtain. The magnitude of the loss coefficient levels measured in the damper and tip regions are generally comparable, which indicates that the three-dimensional effects on loss are about the same and that similar accounting for three-dimensional effects in the two regions can be made. Estimated mean curves through the data indicate that, at the same D, $\overline{\omega}_p$ values for streamlines in the tip and damper flow regions are greater than those for elements unaffected by three-dimensional effects by about 0.06 to 0.08.

It is recognized that D-factor, which is a measure of the blade suction surface velocity decrease, may have little meaning when applied to blade elements that form the wake of the damper. However, the D-factor has proven a useful parameter for estimating loss, and applying it to elements across the damper region gives continuity to the design or analysis procedure.

A second approach to describing the loss in the damper flow region is to determine the increment of loss due to the presence of the damper in the flow. This is attempted from the data of figure 5 by taking the overall $\overline{\omega}_p$ and subtracting an estimated profile-loss coefficient for that blade element without a damper. This estimated profile-loss coefficient is obtained by refairing the radial distribution of $\overline{\omega}_p$ across the damper flow region as if the damper were not present. Associated D-factors were obtained from a similar procedure. Values for blade elements with maximum loss coefficients in damper

region are summarized in table II. From table I, damper geometry parameters of primary interest for correlation with loss are damper thickness and the distance of the damper leading edge from the blade leading edge. Notice that the D-$\overline{\omega}_p$ values estimated for this blade without the damper compare very favorably with the values in figure 6 for those blade elements essentially unaffected by three-dimensional effects.

The data summarized in table II indicate that there is a qualitative trend that the incremental loss due to the damper $\Delta\overline{\omega}_d$ decreases with a reduction in damper maximum thickness t_m and with an increase in distance from the blade leading edge to the damper leading edge d. The larger d value tends to place the damper in a lower Mach number flow regime. However, the data were insufficient to provide a quantitative correlation. Another factor that probably influences the damper loss coefficient $\Delta\overline{\omega}_d$ is how closely the actual flow streamlines compare with design streamlines along which the damper is located. A rough measure of this can be obtained by comparison of the measured values of overall pressure ratio and flow with the design values as shown in figure 4. For example, with rotors 8A and 14A the measured pressure ratio and flow are very close to the design values and the $\Delta\overline{\omega}_d$ values are among the lowest values (0.045 to 0.065) recorded. In comparison, with rotor 3B there is a significant difference between the measured and design operating conditions and the $\Delta\overline{\omega}_d$ is among the highest values (0.103) recorded. This comparison of damper loss indicates an additional factor for consideration in order to minimize damper losses. In summary, the data of table II indicate that for an operating tip speed of 426.7 meters per second (1400 ft/sec) and the listed damper geometry, the increment of loss coefficient due to the damper to be added to the nominally calculated loss coefficient could be in the range of 0.045 to 0.065 with good design practice.

The plots of figure 5 also indicate the spanwise extent of the direct effects of the damper on loss coefficient and the loss gradients over this portion of the span. In general, the $\overline{\omega}_p$ plots indicate that the damper affects the loss over a spanwise distance of approximately 10 times the damper maximum thickness. The maximum effect is immediately downstream of the damper, and the effects decrease in a nearly linear and similar pattern to a zero effect at spanwise locations about ±5 maximum damper thicknesses on either side.

Application of Damper Effects into Typical Aerodynamic Design Procedures

In this section two examples are presented to demonstrate the inclusion of loss gradients across the damper flow region in an aerodynamic design procedure. The first example uses as input the measured radial distributions of energy addition and loss into aerodynamic calculation program and compares calculated with measured parameters. A

second example compares the computed results from two design cases with the same energy addition input but with different loss inputs. In one case the loss input does not account for local damper losses and, in this respect, is typical of current design practices. For the second case the loss input includes the high loss gradient across the damper flow region.

The first example used the data from rotor 3A (fig. 5(a)), and the results are shown in figure 7 on which the computed and measured results are compared. The measured radial distributions of outlet total pressure P_2 and outlet total temperature T_2 (energy addition) were inputs to the computer program. This means, in turn, that the measured radial distribution of loss was utilized. The objective of this example was to demonstrate that, if the actual radial variation of loss across the damper flow region is used, the design program will compute radial distributions of flow conditions closely approximating the actual (measured) flow conditions. The closeness of the computed and measured radial distributions of meridional velocity V_M, diffusion factor D, and outlet absolute flow angle β_2 indicates that this objective is satisfied.

The second example uses the data and geometry of rotor 14A, and the results are plotted in figure 8. The objective of this example was to compare the results of two aerodynamic designs: one applying a typical loss input used in current design procedures that do not account for local damper loss, and a second applying a loss input which does account for local damper loss. The radial distributions of total loss parameter $\overline{\omega}_{tot} \cos \beta_2'/2\sigma$ (fig. 8) shows how the two loss inputs varied. The radial distribution of energy addition (applied as ΔT or T_2 in the design method) was taken from the measured data for rotor 14A (fig. 5) and was the same for both design calculations.

A comparison of the computed results illustrates the direction that differences in radial distribution of parameters of a rotor blade row with and without a damper would take. The magnitude of the differences will, of course, depend on the magnitude of the local loss and turning angle effects of the damper. The radial redistributions of flow V_{M_2}, blade loading D, and flow angle entering a downstream stator row β_2 are all evident from the plots.

For interest, in figure 9, the measured radial distributions of parameters for rotor 14A operating conditions are compared with the computed parameters using a damper loss. It is evident that the inclusion of a damper loss provides a close representation to the actual measured flow distributions.

REMARKS

This study of experimental data from a number of high-speed rotor blades with part-span dampers has indicated the general effects of the dampers on the radial distributions

of flow and performance parameters at the rotor exit. The rotor blade rows used in this study generally covered a relatively narrow range of blade and part-span damper geometry. All data presented were measured at a corrected operating blade speed or approximately 426.7 meters per second (1400 ft/sec). The qualitative effects of the dampers on the radial distributions of rotor flow and performance parameters are clearly defined. These trends should be applicable to any rotor row with a part-span shroud. The magnitude of the damper effects should have direct application to rotor rows with similar geometry and operating conditions. Some care should be used when applying the quantitative results shown herein to rotor rows that differ widely in geometry and operating conditions from those used in the correlation. However, the data shown herein do represent a base for estimating the effects for any rotor row. In any aerodynamic design or analysis calculation that accounts for streamline curvature and radial variations of enthalpy and entropy, an accurate prediction of the radial variation of flow conditions depends on entering into the calculations the correct radial gradients of entropy as well as absolute level. The data presented herein clearly define the distribution of loss across the damper flow region. Applying a similar distribution, even if the magnitude is somewhat in error, to any calculation should result in a radial distribution of flow conditions that more closely approximates the real flow conditions.

Example calculations presented herein have shown that the sharp loss gradients in the damper flow region can be included in an aerodynamic design procedure and that the computed spanwise variations of blade-element parameters compare favorably with measured distributions. The extent that damper effects can be incorporated into blade design procedures has not been explored. Attempts to maintain a pressure rise across the damper region by increasing energy addition sufficiently to match the higher losses could result in an undesirable spanwise distribution of blade camber. Further studies carrying the local damper effects through the complete design system are needed. However, it seems likely that some modest increases in blade camber (to increase energy addition) could be advantageous toward maintaining the pressure rise in the damper region.

CONCLUSIONS

A study of the effects of rotor part-span dampers on rotor blade row operation has been made. Experimental data, including detailed radial surveys of rotor inlet and outlet flow conditions, from eight rotor configurations were used. All rotors had an approximately 50.8-centimeter (20-in.) tip diameter at the rotor leading edge. All rotor configurations had a design blade inlet tip speed of about 426.7 meters per second (1400 ft/sec). This report presents the results for near design operation, that is, at design blade speed and near maximum efficiency operation. From this study the following conclusions are made:

(1) There was a significant increase in loss coefficient in the damper flow regions. For the rotor blade rows used in this study, the maximum loss coefficients in the damper region were from 0.05 to 0.08 higher than those from blade elements outside the damper flow region with the same level of loading. The magnitude of this increase is approximately the same as that observed for blade tip elements (5 percent span height from the tip) where secondary flows result in additional losses. Loss correlation with damper geometry indicated that, qualitatively, the magnitude of damper loss decreased with a reduction in damper maximum thickness and with an increase in distance from blade leading edge to the damper leading edge.

(2) The spanwise distance over which the loss level was directly affected by the damper presence was approximately 10 damper maximum thicknesses. The increase in loss due to the damper generally decreased nearly linearly from the maximum to zero over spanwise distances of ±5 maximum damper thicknesses.

(3) Fluid turning and axial velocity in the damper region were reduced from those observed in adjacent flow regions. The counteracting effects of these two parameters on energy addition were such that there were no significant variations in energy addition across the damper flow region.

(4) The high loss variation across the damper was applied in an aerodynamic design procedure that accounts for radial variations of enthalpy and entropy. The two examples presented showed a close comparison of computed and measured results across the complete blade span including the high entropy gradient damper region.

Lewis Research Center,
National Aeronautics and Space Administration,
Cleveland, Ohio, October 17, 1972,
501-24.

APPENDIX A

SYMBOLS

c	chord length, cm
D	diffusion factor (see eq. (B2))
d	distance from blade leading edge to damper leading edge (fig. 1), cm
M	Mach number
P	total pressure, N/cm^2
$\overline{(P_2/P_1)}$	mass-averaged pressure ratio
p	static pressure, N/cm^2
r	radius, cm
T	total temperature, ^oR
ΔT	total temperature change, ^oR
V	air velocity, m/sec
W	weight flow, kg/sec
w	damper width (fig. 1), cm
α_c	cone angle approximating streamline across blade row, deg
β	air angle, angle between air direction and meridional plane, deg
γ	ratio of specific heats (1.40)
δ	ratio of inlet total pressure to standard pressure of 10.1 N/cm^2 (14.69 psia)
δ^o	deviation angle (eq. (B1)), deg
$\overline{\eta}$	mass-averaged efficiency
θ	ratio of inlet total temperature to standard temperature of 288.2^o K (518.7^o R)
κ_{mc}	angle between blade mean camber line at leading or trailing edge and meridional plane, deg
σ	solidity, ratio of chord to spacing
$\overline{\omega}$	total loss coefficient (eq. (B3))
$\overline{\omega}_p$	profile-loss coefficient (eq. (B4))
$\overline{\omega}_s$	shock-loss coefficient

Subscripts:

d	damper
h	hub
id	ideal
LE	leading edge
M	meridional direction
TE	trailing edge
t	tip
θ	tangential direction
1	inlet measuring or calculation station
2	outlet measuring or calculation station

Superscript:

'	relative to rotor

APPENDIX B

PERFORMANCE PARAMETERS

Deviation angle:

$$\delta^{o} = (\beta')_{TE} - (\kappa_{mc})_{TE} \tag{B1}$$

Diffusion factor:

$$D = 1 - \frac{V'_{TE}}{V'_{LE}} + \frac{(rV_{\theta})_{TE} - (rV_{\theta})_{LE}}{(r_{LE} + r_{TE})\sigma V'_{LE}} \tag{B2}$$

Total loss coefficient:

$$\bar{\omega} = \frac{(P'_{id})_{TE} - P'_{TE}}{P'_{LE} - p_{LE}} = \frac{\left(\frac{P'_{TE}}{P'_{LE}}\right)_{id}\left[1 - \frac{\frac{P_{TE}}{P_{LE}}}{\left(\frac{T_{TE}}{T_{LE}}\right)^{\gamma/(\gamma-1)}}\right]}{\left\{1 - \left[\frac{1}{1 + \frac{\gamma - 1}{2}\left(M'_{LE}\right)^{2}}\right]^{\gamma/(\gamma-1)}\right\}} \tag{B3}$$

Profile loss coefficient:

$$\bar{\omega}_{p} = \bar{\omega} - \bar{\omega}_{s} \tag{B4}$$

Equivalent weight flow:

$$\frac{W\sqrt{\theta}}{\delta} \tag{B5}$$

REFERENCES

1. Hager, Roy D.; Janetzke, David C.; and Reid, Lonnie: Performance of a 1380-Foot-Per-Second-Tip-Speed Axial-Flow Compressor Rotor With A Blade Tip Solidity of 1.3. NASA TM X-2448, 1972.

2. Lewis, George W., Jr.; and Urasek, Donald C.: Comparison of the Effect of Two Damper Sizes on the Performance of a Low-Solidity Axial-Flow Transonic Compressor Rotor. NASA TM X-2536, 1972.

3. Janetzke, David C.; Ball, Calvin L.; and Hager, Roy D.: Performance of 1380-Foot-Per-Second Tip-Speed Axial-Flow Compressor Rotor With Blade Tip Solidity of 1.1. NASA TM X-2449, 1972.

4. Ball, Calvin L.; Janetzke, David C.; and Reid, Lonnie: Performance of a 1380-Foot-Per-Second-Tip-Speed Axial-Flow Compressor Rotor With Blade Tip Solidity of 1.5. NASA TM X-2379, 1972.

5. Kovich, George; and Reid, Lonnie: Overall and Blade Element Performance of a Multiple-Circular-Arc Bladed Transonic Compressor Rotor With Tip Speed of 1375 Feet-Per-Second. NASA TM X-2697, 1972.

6. Moore, Royce D.; and Reid, Lonnie: Performance of a Single-Stage Axial-Flow Transonic Compressor Stage With a Blade Tip Solidity of 1.7. NASA TM X-2658, 1972.

7. Urasek, Donald C.; Moore, Royce D.; and Osborn, Walter M.: Performance of a Single-Stage Transonic Compressor With a Blade-Tip Solidity of 1.3. NASA TM X-2643, 1972.

8. Schwenk, Francis C.; Lewis, George W.; and Hartmann, Melvin J.: A Preliminary Analysis of the Magnitude of Shock Losses in Transonic Compressors. NACA RM E57A30, 1957.

TABLE I. - SUMMARY OF ROTOR BLADE DAMPER GEOMETRY

[With the exception of rotor 3A, typical damper geometry were as follows: aerodynamic chord of damper, approximately 30 percent of aerodynamic chord of blade; maximum thickness of the damper, 15 percent of aerodynamic chord of damper and located at midchord; leading and trailing edge radii, set equal to 0.25 cm (0.010 in.); inner and outer surfaces of the damper, circular arc shapes.]

Rotor	Rotor aerodynamic chord, c, cm	Damper maximum thickness, tm, cm	Distance from blade leading edge to damper leading edge, d, cm (a)	Damper width, w, cm (a)	$\frac{tm}{c} \times 100$, percent (a)	$\frac{d}{c} \times 100$, percent (a)	$\frac{w}{c} \times 100$, percent (a)	Reference reports
3A	4.48	0.32	1.25	2.95	7	28	66	1
3B	4.48	.19	1.54	1.15	4	34	26	2
4A	3.76	.19	1.25	1.13	5	33	30	3
5A	4.96	.19	1.77	1.18	4	36	24	4
6A	4.42	.19	1.53	1.20	4	34	27	5
8A	4.71	.21	1.45	1.82	4	31	39	--
12A	4.72	.21	1.57	1.59	4	33	34	6
14A	4.70	.21	1.32	2.07	4	28	44	7

[a]All values in rotor chord direction (see fig. 1).

TABLE II. - SUMMARY OF PROFILE LOSS COEFFICIENTS IN DAMPER FLOW REGION

Rotor	Maximum measured profile-loss coefficient, $\bar{\omega}_p$, with damper	Estimated $\bar{\omega}_p$ without damper	Incremental $\bar{\omega}_p$ due to damper	D-factor with damper	Estimated D-factor without damper	Damper maximum thickness, tm, cm	Distance from blade leading edge to damper leading edge, d, cm
3A	0.190	0.052	0.138	0.630	0.555	0.32	1.25
3B	.138	.035	.103	.572	.530	.19	1.54
4A	.123	.037	.086	.560	.502	.19	1.25
5A	.088	.023	.065	.553	.530	.19	1.77
6A	.133	.060	.073	.622	.570	.19	1.53
8A	.108	.062	.046	.540	.528	.21	1.45
12A	.158	.070	.088	.582	.540	.21	1.57
14A	.110	.045	.065	.568	.545	.21	1.32

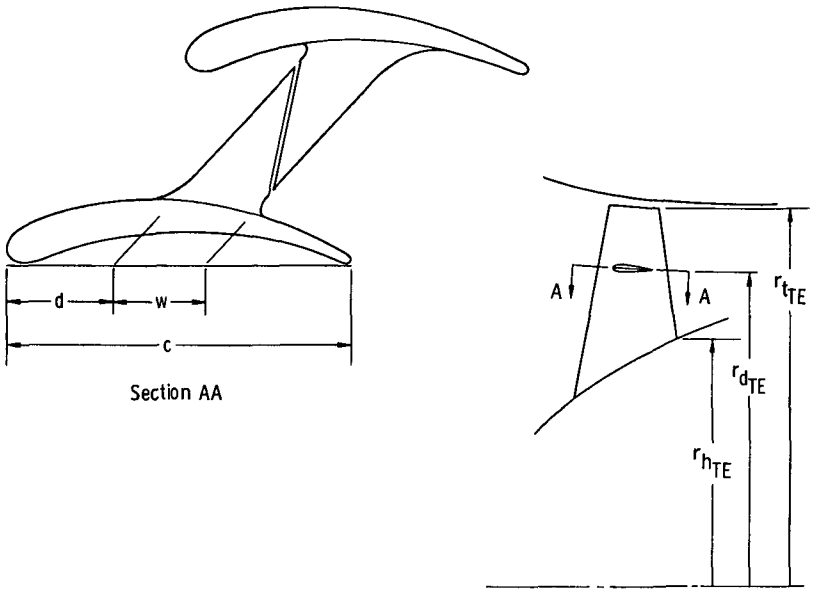

Figure 1. - Blade with part-span damper defining damper geometry parameters.

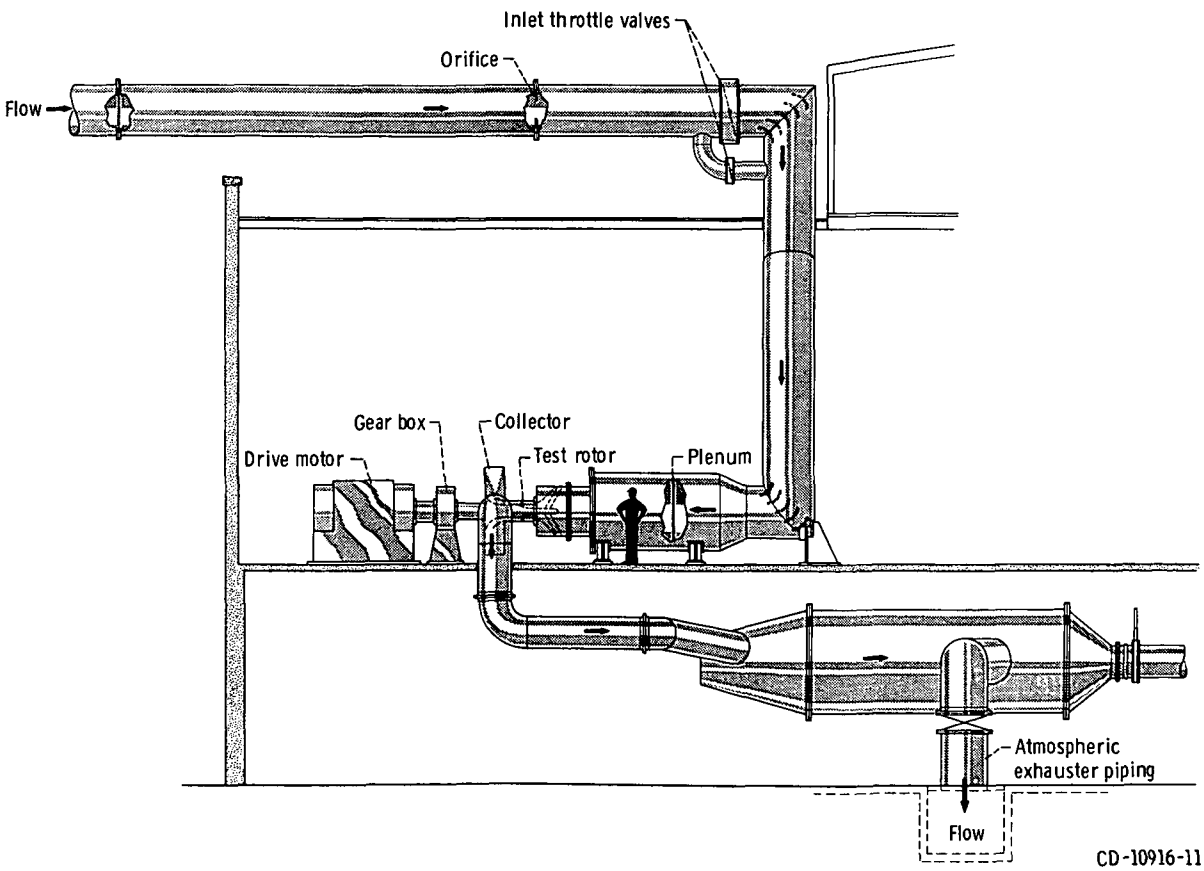

Figure 2. - Test facility.

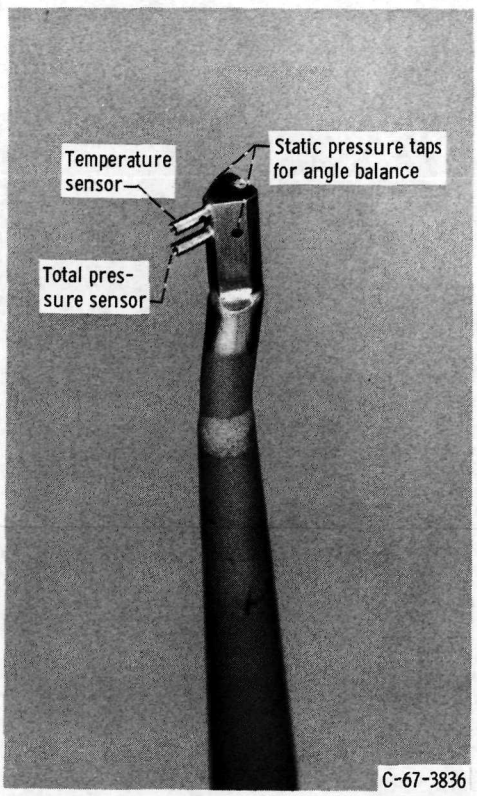

(a) Combination total pressure, total temperature, and flow angle probe (double barrel).

(b) Static pressure probe (C type; $7\frac{1}{2}^{o}$ wedge).

Figure 3. - Typical probes which measures static and total pressures, total temperatures, and flow angle.

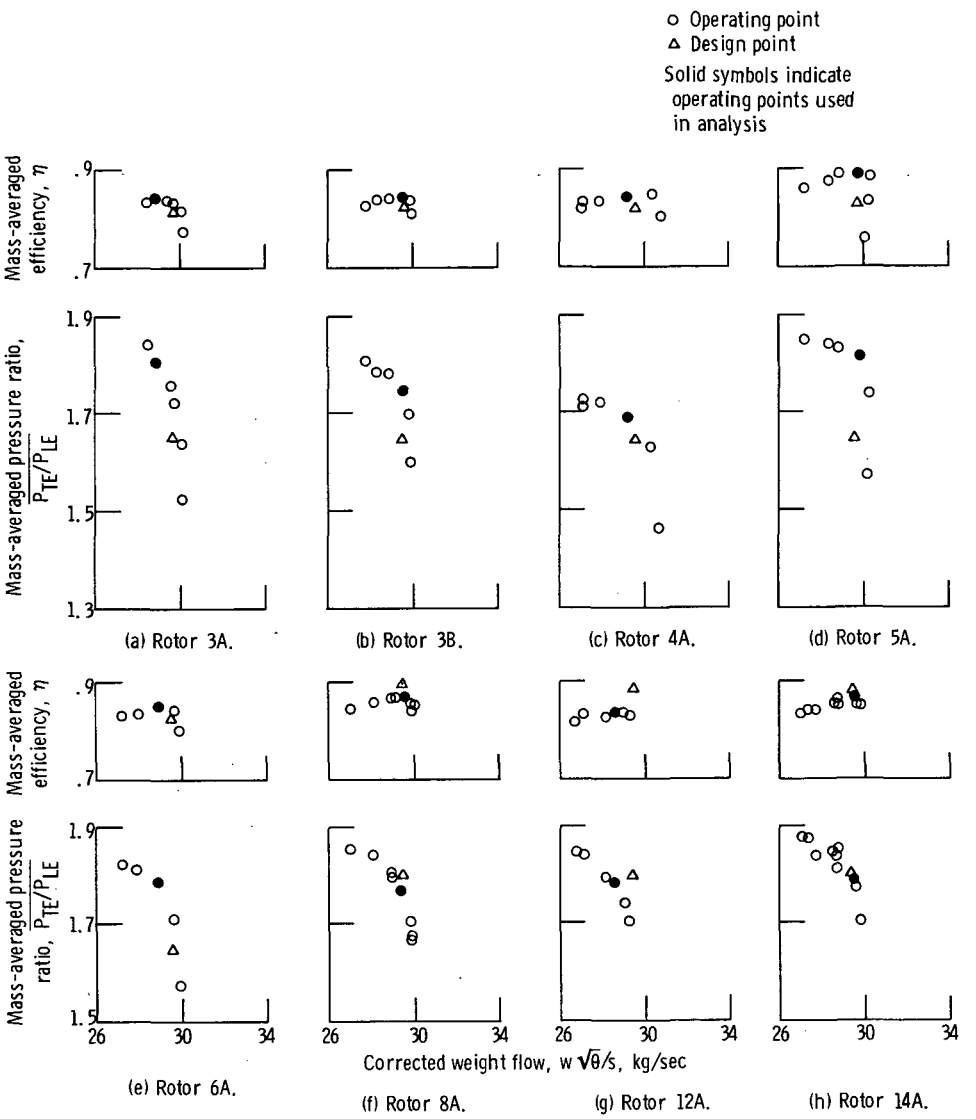

Figure 4. - Overall performance of eight rotors.

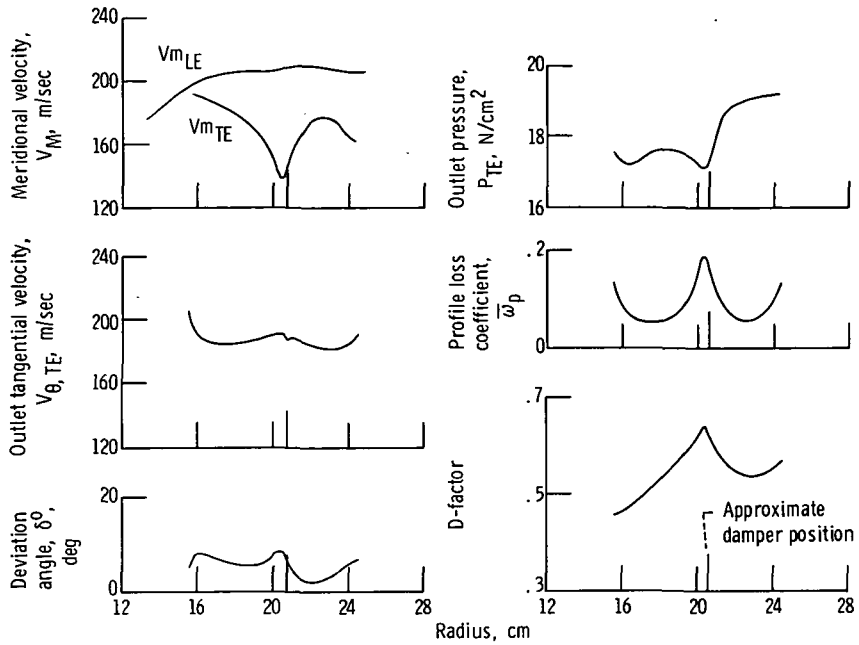

(a) Rotor 3A; reading 532.

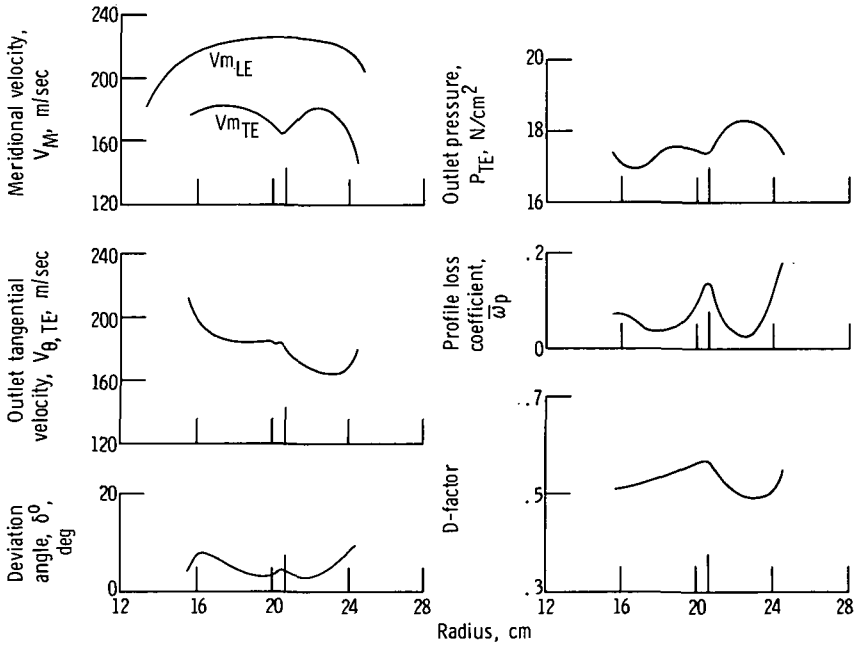

(b) Rotor 3B; reading 20.

Figure 5. - Blade-element data.

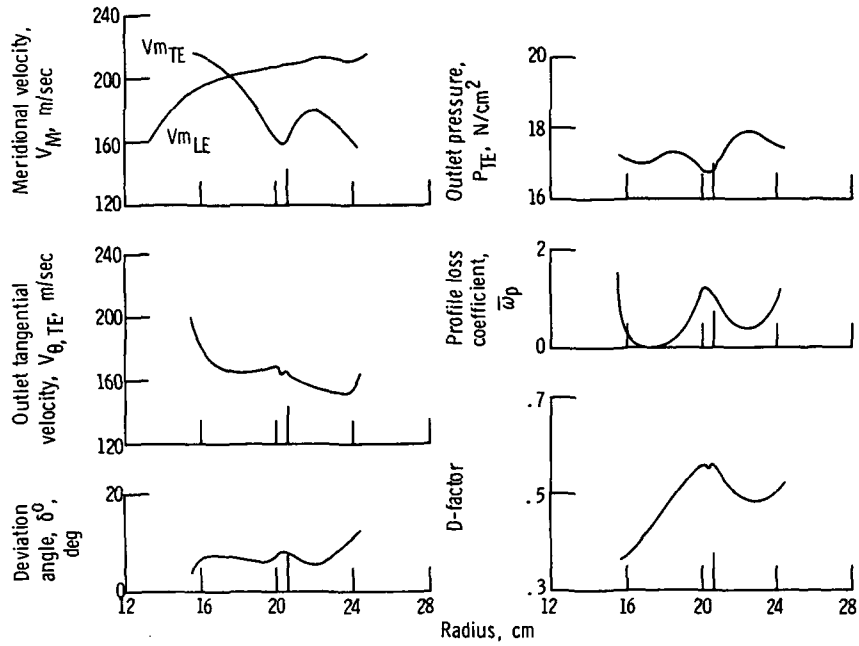

(c) Rotor 4A; reading 919.

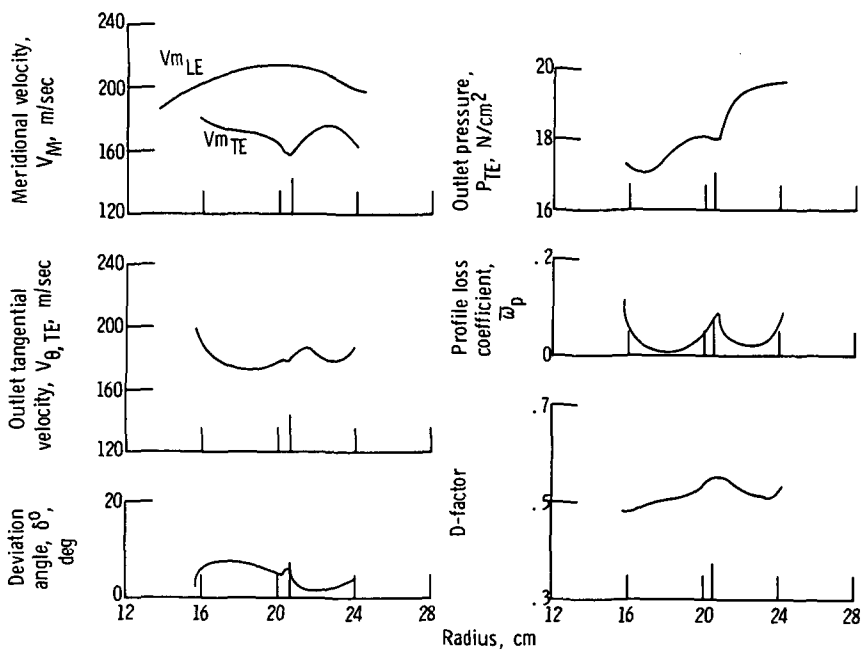

(d) Rotor 5A; reading 992.

Figure 5. - Continued.

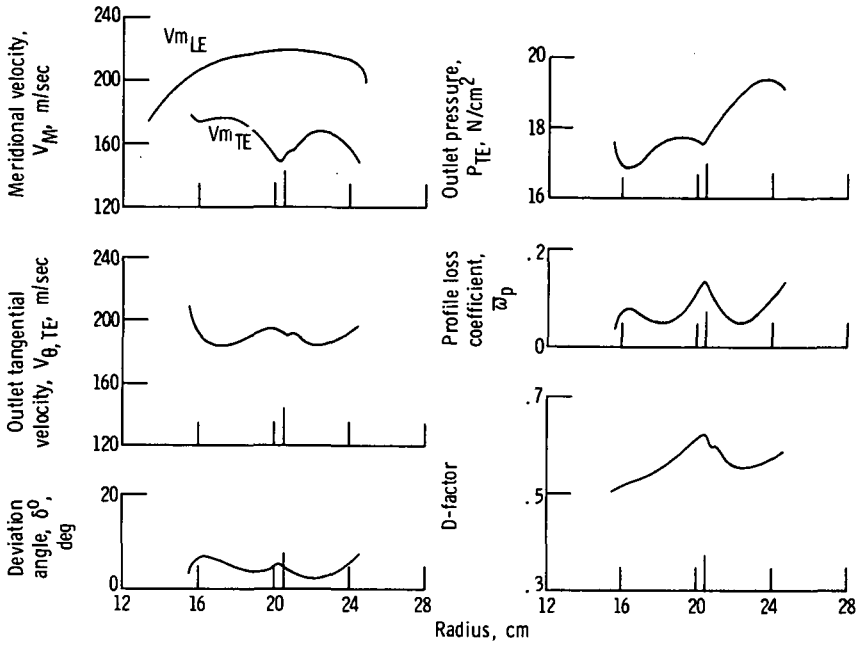

(e) Rotor 6A; reading 198.

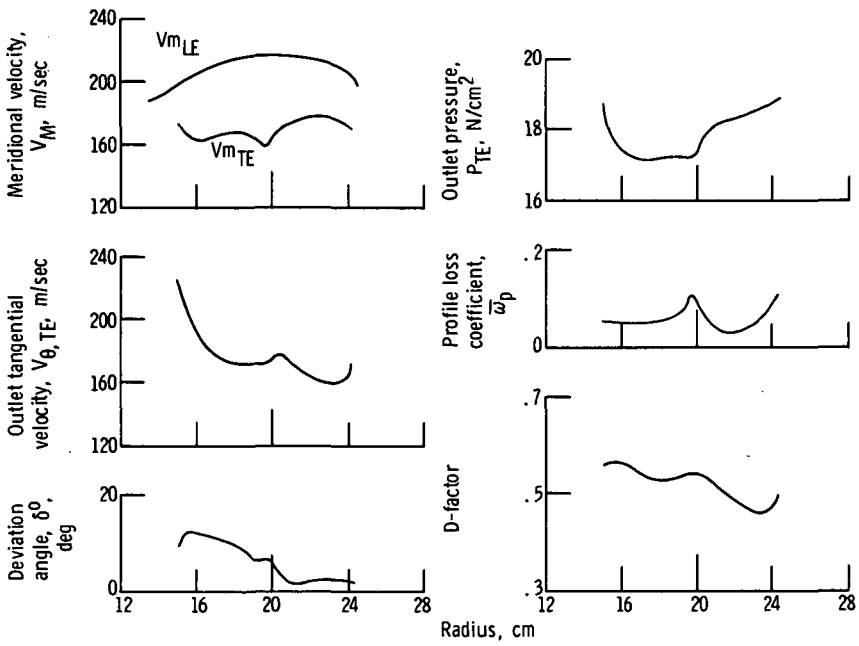

(f) Rotor 8A; reading 59.

Figure 5. - Continued.

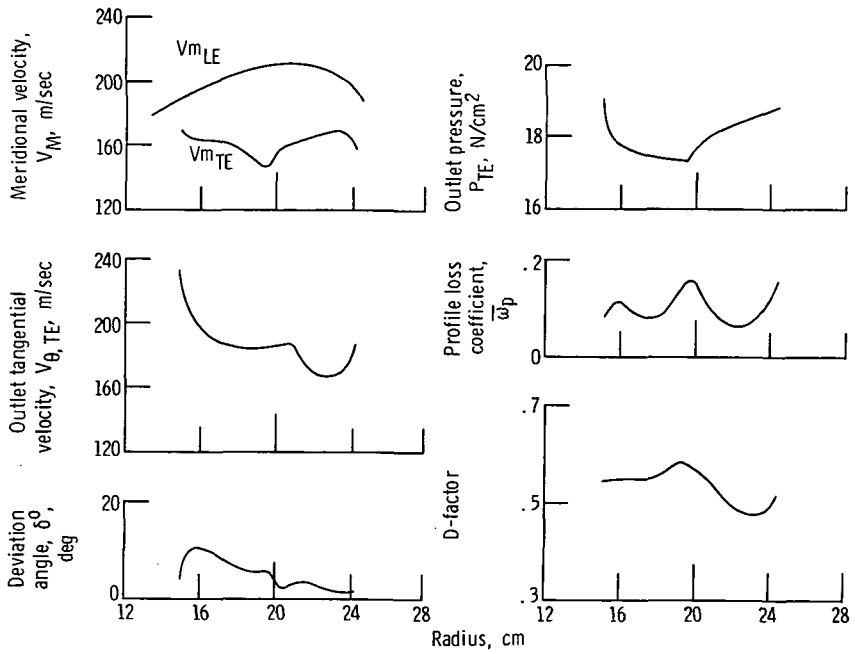

(g) Rotor 12A; reading 305.

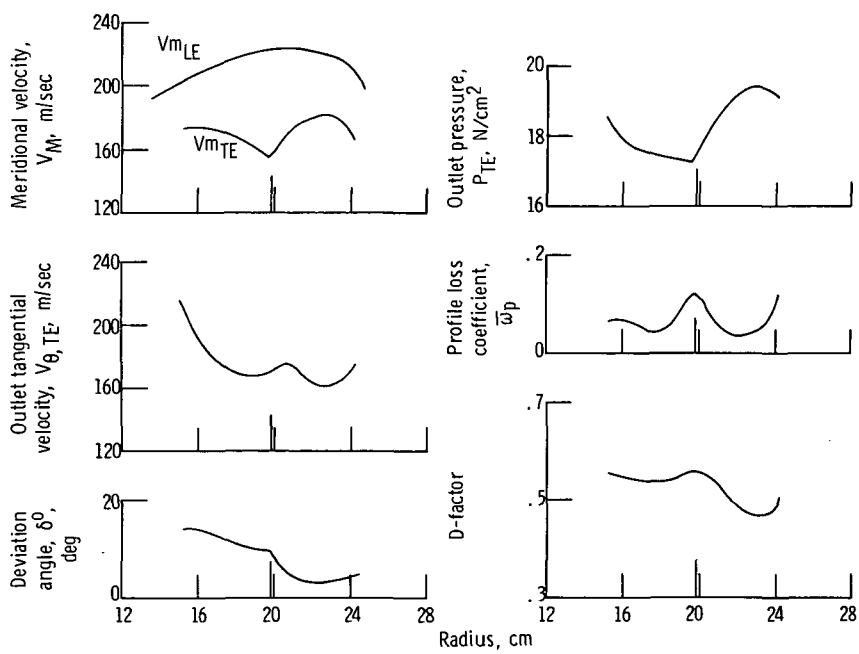

(h) Rotor 14A; reading 341.

Figure 5. - Concluded.

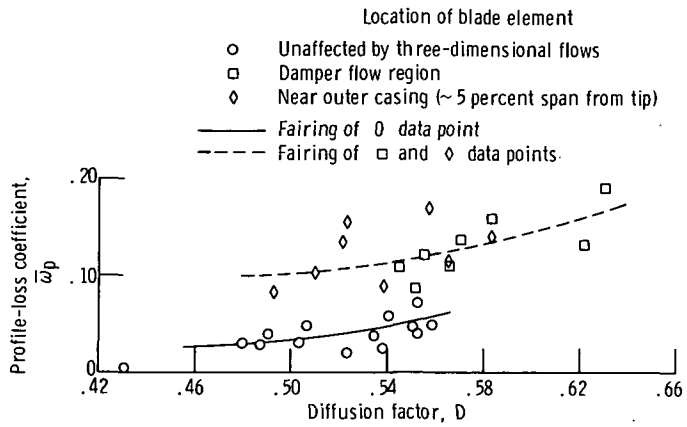

Figure 6. - Correlation of loss with blade loading parameter.

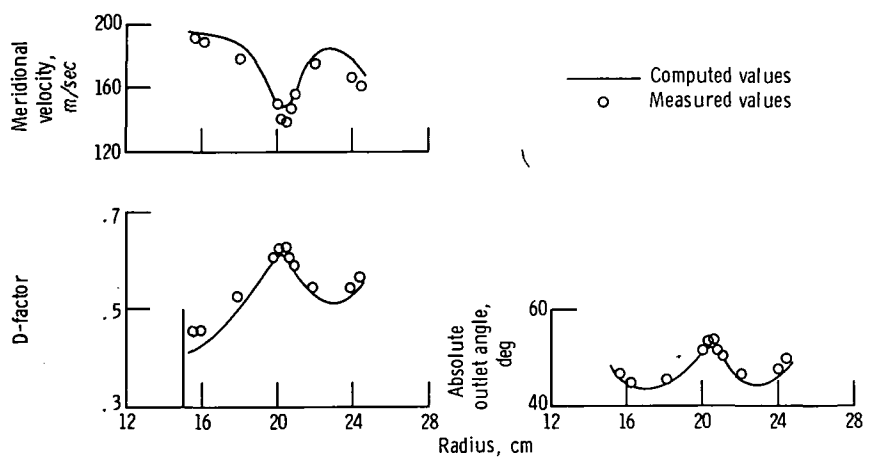

Figure 7. - Comparison of measured and computed parameters using measured values of loss and energy addition in aerodynamic design procedure.

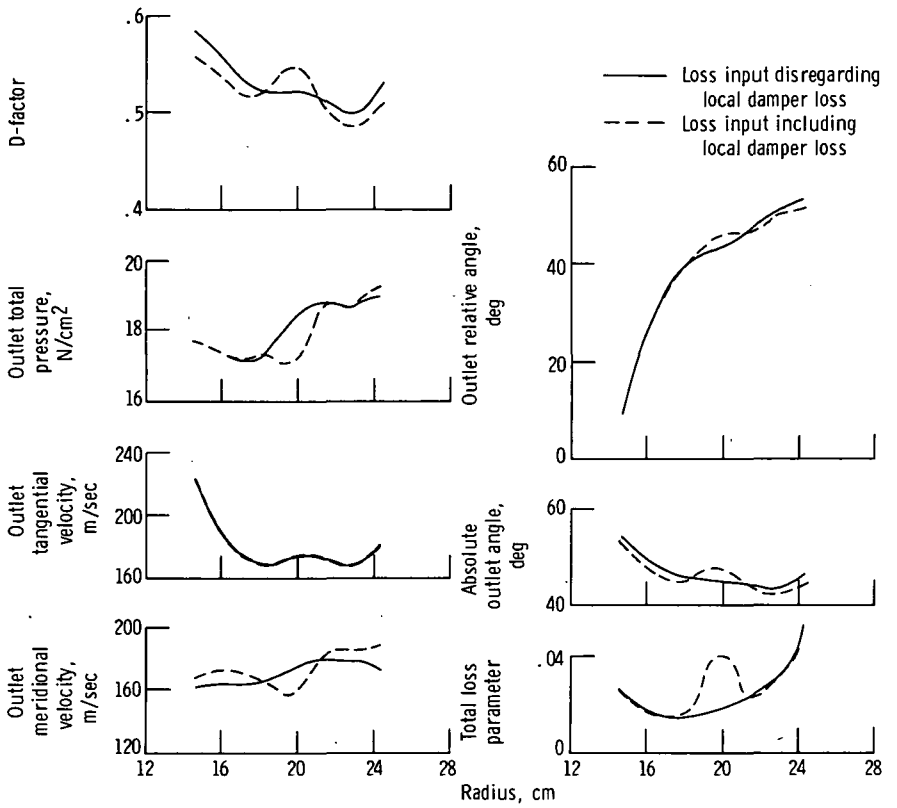

Figure 8. - Comparison of computed parameters using same energy addition with two different loss inputs.

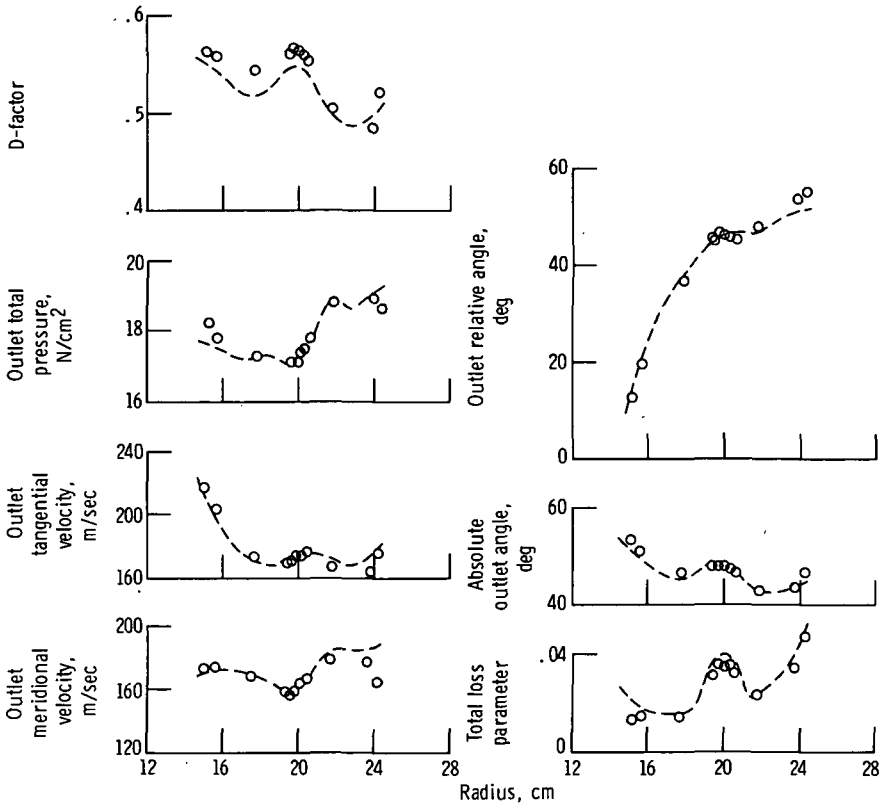

Figure 9. - Comparison of measured parameters with computed values using measured energy addition and losses including local damper loss.

NATIONAL AERONAUTICS AND SPACE ADMINISTRATION
WASHINGTON, D.C. 20546

OFFICIAL BUSINESS
PENALTY FOR PRIVATE USE $300

SPECIAL FOURTH-CLASS RATE BOOK

POSTAGE AND FEES PAID
NATIONAL AERONAUTICS AND SPACE ADMINISTRATION
451

U.S.MAIL

POSTMASTER: If Undeliverable (Section 158 Postal Manual) Do Not Return

"The aeronautical and space activities of the United States shall be conducted so as to contribute . . . to the expansion of human knowledge of phenomena in the atmosphere and space. The Administration shall provide for the widest practicable and appropriate dissemination of information concerning its activities and the results thereof."

—NATIONAL AERONAUTICS AND SPACE ACT OF 1958

NASA SCIENTIFIC AND TECHNICAL PUBLICATIONS

TECHNICAL REPORTS: Scientific and technical information considered important, complete, and a lasting contribution to existing knowledge.

TECHNICAL NOTES: Information less broad in scope but nevertheless of importance as a contribution to existing knowledge.

TECHNICAL MEMORANDUMS: Information receiving limited distribution because of preliminary data, security classification, or other reasons. Also includes conference proceedings with either limited or unlimited distribution.

CONTRACTOR REPORTS: Scientific and technical information generated under a NASA contract or grant and considered an important contribution to existing knowledge.

TECHNICAL TRANSLATIONS: Information published in a foreign language considered to merit NASA distribution in English.

SPECIAL PUBLICATIONS: Information derived from or of value to NASA activities. Publications include final reports of major projects, monographs, data compilations, handbooks, sourcebooks, and special bibliographies.

TECHNOLOGY UTILIZATION PUBLICATIONS: Information on technology used by NASA that may be of particular interest in commercial and other non-aerospace applications. Publications include Tech Briefs, Technology Utilization Reports and Technology Surveys.

Details on the availability of these publications may be obtained from:

SCIENTIFIC AND TECHNICAL INFORMATION OFFICE

NATIONAL AERONAUTICS AND SPACE ADMINISTRATION

Washington, D.C. 20546